

15 **ABSTRACT**

16 The increase in urban runoff brought about by a rise in impermeable surfaces has
17 triggered the alteration and pollution of many aquatic systems. The overall goal of this
18 research was to design a ‘Sustainable Urban Drainage System’(SUDS) for the retention of
19 heavy metals from a car park consisting of mixing autochthonous soil (70%) with sand
20 (30%) to improve the hydrological conductivity and adsorption capacity. To quantify the
21 retention of metals we characterize the adsorption kinetics and isotherms of the soil mixture
22 and perform dynamic experiments. The proposed methodology allowed us to work out the
23 amount of heavy metal retention by the adsorbent and the retention mechanisms. The
24 retention capacity of the adsorbent mixture was as follows: $\text{Cr}^{3+} \approx \text{Cu}^{2+} \gg \text{Zn}^{2+} > \text{Ni}^{2+} >$
25 Cd^{2+} . Chromium and copper ions were mainly retained by precipitation, whereas zinc,
26 nickel and cadmium were retained by ionic exchange with calcium ions that saturate the
27 soil colloids. The soil mixture buffered pH was found to change when fed with an acid
28 solution of metallic ions.

29

30 **Keywords:** Heavy metal adsorption, Stormwater runoff, Sustainable Urban Drainage
31 Systems (SUDS), Car park stormwater.

32 1 INTRODUCTION

33 The increase in impermeable surfaces due to urban development alters the urban
34 hydrological cycle, augmenting surface runoff as well as the frequency and magnitude of
35 floods and the pollution of surface aquatic systems (Göbel *et al.*, 2007; Hatt *et al.*, 2006,
36 2009; Hou *et al.*, 2019; Li *et al.*, 2009). Urban runoff water pollution is normally linked to
37 anthropogenic activities like vehicle traffic, industrial activity and street cleaning (Barbosa
38 *et al.*, 2012; Huber *et al.*, 2016). At present, the discharges of this water are considered
39 diffuse or nonpoint-source pollution (Fuerhacker *et al.*, 2011; Ma *et al.*, 2018).

40 The nature and origin of runoff water contamination is highly variable. Most studies
41 identify urban water contaminants as solids in suspension (SS), soluble salts, heavy metals
42 (Cu, Zn, Cd, Pb, Ni and Cr), pesticides, nutrients from fertilizers, biodegradable organic
43 matter, polycyclic aromatic hydrocarbons (PAHs), and pathogenic microorganisms. All
44 these pollutants contribute to water quality degradation (Barbosa *et al.*, 2012; Bressy *et al.*,
45 2012; Göbel *et al.*, 2007; Tedoldi *et al.*, 2016).

46 The amount and characteristics of the pollutant load are affected by hydrological
47 factors, such as rainfall intensity, duration, and intervals between rainfall events. They are
48 also affected by vehicle traffic movement (in car parks or in the street), industrial activity,
49 or the maintenance of green spaces (Crabtree *et al.*, 2006; Helmreich *et al.*, 2010; Lee *et al.*,
50 2004). Another important aspect is the way in which the contaminants are transferred
51 from one place to another, either dissolved or adsorbed to particles. This, together with the
52 release of coarser particles in pavings, has been the subject of specific studies such as those
53 by Borris *et al.* (2016); Helmreich *et al.* (2010); Huber *et al.* (2016).

54 One of the urban spaces with greater impacts on the quality of urban runoff water are
55 public car parks, particularly those in high demand areas like in large commercial spaces,
56 hospitals or universities. These surfaces generate large quantities of heavy metals and
57 hydrocarbons (Gnecco *et al.*, 2019; Huber *et al.*, 2016; Monrabal-Martinez *et al.*, 2019;
58 Salim Akhter & Madany, 1993; Schiff *et al.*, 2016).

59 A number of techniques have been developed in order to improve urban runoff water
60 management form areas like car parks. These have been given different terms, like “Low
61 Impact Development (LID)”, “Water Sensitive Urban Design (WSUD)” or “Sustainable
62 Urban Drainage Systems (SUDS)” (Fletcher *et al.*, 2015). In this work we focus on SUDS,

63 which constitute a set of tools that aim to reproduce the natural conditions of urban runoff
64 reducing the hydrological impact of urban design, facilitating infiltration where the
65 terrain's conditions permit it, controlling the excess rainwater, and transferring it slowly to
66 water areas (Andrés-Doménech *et al.*, 2018; Charlesworth *et al.*, 2012; Dietz and Clausen,
67 2008; Eckart *et al.*, 2017). These systems have proven effective in the management of
68 suspended sediments, heavy metals and nutrients (Davis *et al.*, 2001; Jia *et al.*, 2015; Zinger
69 *et al.*, 2007).

70 The efficiency of SUDS to remove heavy metals from runoff water depends on
71 several factors, among them the adsorption capacity and hydraulic conductivity of the
72 surface medium, runoff first flush volume and composition, as well as the presence of
73 vegetation that prevents clogging and erosion (Allabashi *et al.*, 2019; Flanagan *et al.*, 2019;
74 Kandra *et al.*, 2014; Tedoldi *et al.*, 2016; Tedoldi *et al.*, 2017b). A comprehensive analysis
75 of different factors controlling heavy metal pollution from urban runoff is presented in
76 previous reviews (Eckart *et al.*, 2017; Huber *et al.*, 2016; Kabir *et al.*, 2014; Tedoldi *et al.*,
77 2016; Vardhan *et al.*, 2019).

78 The soil hydraulic characteristics of the SUDS may vary depending on their function.
79 In general, the medium should have enough permeability to prevent permanent
80 waterlogging, but it should be low enough for the system to be capable of adsorbing the
81 contaminants that it receives (Le Coustumer *et al.*, 2012). Another factor in SUDS design
82 is the balance between the adsorption efficiency of the material and its economic and
83 environmental cost. Local materials should be preferred for reducing transport costs and
84 carbon footprint.

85 It is of great importance to make an exhaustive study of the bed material in order to
86 determine its future behaviour as a pollutant load retainer. Faced with this challenge, a
87 number of questions arise, both at a design and at a maintenance level. At a design level:
88 What type of adsorbent is the most adequate for retaining the largest amount of heavy
89 metals while maintaining an infiltration intensity? What characteristics should it have?
90 With respect to maintenance: What pollutant load (heavy metals) can the soil retain? How
91 much runoff can be managed? What lifespan can the medium have before causing problems
92 for the environment?

93 Thus, the main objective of this research is to answer these questions, that is, to

94 determine the heavy metal retention capacity of a given type of medium or soil for a SUDS.
95 To define the medium, an autochthonous soil from the site has been employed and three
96 types of sand tested to improve infiltration conditions. Thus, the specific objectives were
97 as follows: (a) to obtain the kinetics and the sorption isotherms of the metals in the soil and
98 in the three types of sand, (b) to select an adsorbent bed with appropriate hydraulic
99 conductivity and retention capacity, (c) to determine the breakthrough curves in dynamic
100 retention assays, and (d) to identify the retention mechanisms of the metals in the filter bed.
101 To explore these questions, we identified an effective medium for the design of a SUDS
102 pilot project in the car park of the Public University of Navarre (UPNA) campus in Tudela
103 (Spain). This SUDS aims to be a prototype for interventions in other places or with other
104 pollutants. For this we develop a methodology for evaluating the system and reach a
105 balance between hydraulic conductivity and adsorption capacity of heavy metals in the
106 runoff water, particularly: Cd^{2+} , Cr^{3+} , Cu^{2+} , Ni^{2+} and Zn^{2+} .

107 **2 MATERIAL AND METHODS**

108 **2.1 Materials and reagents**

109 The soil was obtained from a plot near the SUDS project located in Tudela (Navarre-
110 Spain). The project involved the transformation of a traditional urban stormwater drainage
111 system from the car park into a SUDS (Fig. SII). Samples from the top 30-cms of surface
112 soil were collected in four different areas in the plot. The samples were dried in a laboratory
113 at room temperature for two weeks until a constant mass was obtained, then sieved through
114 a 2 mm mesh. According to the USDA soil taxonomy the soil was classified as *Typic*
115 *Calciustept* and the soil texture distribution was as follows: clay, 28.7% ($< 2 \mu\text{m}$); silt,
116 48.5% ($2 - 20 \mu\text{m}$); sand, 22.8% ($> 50 \mu\text{m}$). To select a type of sand which could improve
117 the soil's infiltration capacity, three commercial sand-types were compared: one of them
118 was river sand (RS) with a heterogeneous particle size, in which coarse grains of different
119 shapes and brownish-coloured fines were observed; the other two were washed sands
120 (WS), which differed in their granulometry (WS₁, with a granulometry between 0.2 and 1.0
121 mm; and WS₂, with a granulometry between 1.0 and 2.0 mm). The saturated hydraulic
122 conductivity of the different types of sand were measured using the constant head method
123 established in the ASTM 2434-68 (2006) standard.

124 2.2 Chemical characterization of the adsorbents

125 The pH was measured under saturated paste conditions (Jackson and Beltrán
126 Martínez, 1982). For this, samples of the adsorbent mixture were placed in 50 mL beakers,
127 to which deionized water was added until a paste was obtained. The ζ -Zeta was determined
128 by photon correlation spectrometry (Malvern model Zetasizer 3000), with an He-Ne laser
129 of 633 nm wavelength and a maximum power of 10 mW. To measure the size of the
130 colloids, approximately 3 mL of leachate was added to standard polystyrene cuvettes. The
131 Zeta-potential was obtained from measurements of the electrophoretic mobility using 50
132 mm quartz capillary cells (Mulligan *et al.*, 2001). For each adsorbent, 200 mg of sample
133 and 25 mL of deionized water were added to a 50-mL centrifuge tube. The tubes were
134 subsequently shaken with the solids and the water, and they were centrifuged at 3000 rpm
135 for 2 minutes in order to separate the largest sized colloidal particles that might interfere in
136 the reading (Mulligan *et al.*, 2001).

137 The inorganic carbon concentration influences the pH of the adsorbent which, in turn,
138 affects the material's retention capacity. The inorganic carbon was determined from the
139 content of CaCO₃ in the soils following the Loeppert *et al.* (1984) procedure.

140 2.3 Adsorption kinetics and isotherms

141 To determine the equilibrium time, 200.0 ± 0.3 mg aliquots of the adsorbent were
142 placed in 50 mL centrifuge tubes (García *et al.*, 1996). To each tube we added 0.25 mL of
143 1.0 M NaNO₃ solution and 25 mL of a metal solution of a known concentration (Table
144 SI1). The centrifuge tubes were kept at 25.0 ± 0.1 °C under continuous agitation. When the
145 established times (1, 2, 3, 4, 5, 6, 12 and 24 h) elapsed the suspensions were filtered and
146 100 μ L of HNO₃ was added to prevent the hydrolysis of the cations (Echeverría *et al.*,
147 1998). The concentration of metals in the filtrate was determined by Atomic Absorption
148 Spectroscopy (ASS) (García *et al.*, 1996; Oliveira *et al.*, 2007). The amount of metal sorbed
149 by the adsorbent was found from the difference between the initial concentration and the
150 concentration in the solution.

151 The adsorption isotherms of Cd²⁺, Cu²⁺, Ni²⁺ and Zn²⁺ were obtained by adding 25
152 mL of an appropriate metal solution to 200 mg of each adsorbent in 50 mL centrifuge tubes.
153 The metal solutions were prepared by diluting 1.000 g L⁻¹ of a standard solution (Titrisol™
154 – Merck) in deionized water. The initial concentrations of the metal solutions were

155 increased to reach the isotherm monolayer. The maximum initial concentration for each
156 ion and adsorbent is shown in Table SI2. The centrifuge tubes were maintained at 25 ± 0.1
157 °C and agitated for 24 h with a frequency of 5 oscillations per second. Then the suspensions
158 were filtered, acidified with 100 μ L of HNO₃ and the concentration of metal was analysed
159 in the supernatant by ASS. A blank was prepared including 200 mg of the soil-sand mixture
160 and 25 mL of deionized water.

161 The adsorption parameters were determined using the models of Langmuir and
162 Freundlich (Ahalya *et al.*, 2003). Although Langmuir's (1918) model assumes a series of
163 premises that are difficult to meet in the case of adsorption in a solution, it allows the
164 deduction of the capacity of the monolayer (Veith and Sposito, 1977), where the amount
165 adsorbed, n^a , is expressed by,

$$n^a = \frac{n_m^a B_L c_e}{1 + B_L c_e} \quad (1)$$

166 where n_m^a represents the concentration of adsorbate corresponding to the covering of the
167 monolayer; B_L is a coefficient of adsorption related to adsorption enthalpy; and C_e is the
168 concentration in equilibrium.

169 Despite its empirical origin and applications (Ahalya *et al.*, 2003), the Freundlich
170 model is rigorous in the sorption to heterogeneous surfaces (Sposito, 1980). Its general
171 expression is as follows:

$$n^a = k_F c_e^n \quad (2)$$

172 where k_F is the Freundlich parameter related to the adsorption capacity and is equivalent to
173 the amount retained for an equilibrium concentration equal to unity; and n is an
174 adimensional parameter. The coefficients were determined through the logarithmic
175 transformation of Equation (2).

176 **2.4 Dynamic column assays of metal retention**

177 Due to the limited saturated hydraulic conductivity of the the soil collected from the
178 sampling plots, an adsorbing bed was prepared from a mixture of soil (70%) and washed
179 sand WS₁ (30%), which combined the original soil's metal retention capacity with the
180 permeability of the sand. The WS₁ sand was selected because of the smaller size of its
181 particles. The assays were made with a glass column having a porous disc at the bottom,

182 also made of glass, as a support for the adsorbent (Fig. 1). The column was 432 mm long
183 with a diameter of 34 mm. The sand/soil mixture or adsorbent was added to the column
184 until reaching a height of 200 mm in all the assays. Next, the adsorbent was compacted
185 with a vibrator (Tecnokartell model TK3S). Given that the height of the material in the
186 column diminished due to vibration, the filling and compacting process was repeated until
187 filling the height of 200 mm pre-established in these tests. Cotton was placed on top of the
188 adsorbent material to prevent erosion and splashing of the adsorbent during the dosing of
189 the solution. To condition the material, and for the first washing of the adsorbent, 200 mL
190 of deionized water was added after packing.

191 400 mL of a 10 mM solution of each metal ion (Cd^{2+} , Cr^{3+} , Cu^{2+} , Ni^{2+} and Zn^{2+}) was
192 added to the column. The solution had been previously adjusted to pH 3 in order to prevent
193 the precipitation of the metal ions in the solution. The concentration of this aqueous
194 solution was high enough for the assays to be completed with a single application of the
195 solution. Therefore, it was much higher than the concentrations that are typical in a parking
196 lot with a high intensity of motor vehicles (Göbel *et al.*, 2007). The metal solution was
197 dosed with a pump (ProMinent Model Beta/5) at pumping conditions of a 30% run and
198 20% pulsation. These conditions were chosen taking into account the hydraulic
199 conductivity of the material/mixture and the pump's characteristics achieving an average
200 inflow rate of 5.5 mL/min.

201 Aliquots of 30 mL were taken from the drained solution at the outlet of the column
202 in order to measure the zeta-potential, the pH and the concentration of ions in the solution
203 (Alcántara *et al.*, 2012). After adding 400 mL of the 10 mM solution of each metal ion, the
204 column was washed with 200 mL of deionized water to eliminate the remains of the
205 solution retained in the pores of the adsorbent (Hatt *et al.*, 2008). The pump's dosing
206 conditions were the same as those described in the previous stage and the leaching samples
207 were collected in the same way as described in the above paragraph.

208 The zeta potential was determined as described in Section 2.2 and the leaching pH
209 was measured with a Metrohm pHmeter and a combined electrode. After measuring the pH
210 of each aliquot, 100 μL of concentrated HNO_3 was added to prevent hydrolysis and
211 precipitation processes in the metal ions (Davis *et al.*, 2001).

212 The concentration of metals in dissolution was determined, either directly or after

213 dilution, by atomic absorption spectroscopy (Perkin-Elmer model 2100). An air-acetylene
214 flame was used and the flows were 2.5 L min⁻¹ of air and 8 L min⁻¹ of acetylene (Davis *et*
215 *al.*, 2001; Fuerhacker *et al.*, 2011; Garcia *et al.*, 1996; Oliveira *et al.*, 2007). The presence
216 of Ca²⁺ in the leaching was also analysed to find out whether any metals were retained due
217 to ion exchange (Singh and Sekhon, 1983).

218 Once the adsorbent was washed, some aliquots were taken from the adsorbent bed in
219 order to measure the distribution of the ions retained throughout the column. Samples were
220 taken from each 5 cm layer of the filter bed (Fig. SI2) and were dried in an oven at 105 °C
221 until a constant mass was obtained (Hatt *et al.*, 2008). Once dried, we added 1,000 ± 0.3
222 mg of each portion to 100 mL Erlenmeyer flasks, together with 6 mL of 60% HNO₃ and 4
223 mL of 36.5% HCl (Ahalya *et al.*, 2003; Davis *et al.*, 2001; Garcia *et al.*, 1996). We included
224 another Erlenmeyer flask containing 1,000 mg of the original soil-sample mixture as a
225 blank. The flasks were placed on hotplates with constant agitation and the samples were
226 kept boiling under reflux for 1 hour (Fig. SI3). Then the samples were cooled, the
227 supernatant filtered into a 100 ml volumetric flask and the content of the flasks was made
228 up to the mark with deionized water. Cation concentrations in the extracts were determined
229 by AAS as was described above (Garcia *et al.*, 1996; Oliveira *et al.*, 2007).

230 Given that the column infiltration was under laminar flow conditions, the hydraulic
231 conductivity, k_s , was determined from the Darcy equation by measuring the flow at the
232 column outlet and the increase in hydraulic load between the entry and exit points of the
233 adsorbent medium in the column. A digital manometer (Keller LEO 1) was placed at the
234 upper part of the column to measure the hydraulic load. The hydraulic properties of the
235 WS₁ sand and of the mixture of soil/sand were determined in triplicate.

236 **3 RESULTS AND DISCUSSION**

237 **3.1 Characterization of adsorbent material**

238 Table 1 shows the inorganic carbon content, expressed as a percentage of calcium
239 carbonate, the pH and the zeta potential. The inorganic carbon content ranged from 34.9%
240 for soil to 0.38% for washed sands. The carbonate content is related to the origin of each
241 of the samples. The soil comes from an arid zone, which is rich in calcium carbonate. The
242 scarce percentage of carbonates in the WS₁ and WS₂ sand samples could be due to washing

243 prior to their commercialization. Therefore, on the basis of the inorganic carbon content in
244 the samples, the soil had a greater capacity than sand samples to buffer the pH and favour
245 the retention of metal ions.

246 The pH was basic in all the cases, with values between 7.9 for the soil and 8.7 for the
247 WS₁ sand sample. The values of ζ-Zeta obtained in the assays for the four materials
248 analysed were around -20.0 mV, a favourable potential for the retention of metal cations in
249 solution. There were no significant differences between the values of ζ-Zeta in the samples
250 analysed.

251 3.2 Sorption kinetics and isotherms of the metal ions

252 Figure 2 shows the sorption of Cd²⁺, Cr³⁺, Cu²⁺, Ni²⁺ and Zn²⁺ by the soil and the
253 three sand-types as a function of time. Due to the different adsorption capacity of the soil
254 and sand samples, the amount of retained metal is expressed as a percentage with respect
255 to the initial concentration in solution. We kept the adsorbent-mass/solution-volume ratio
256 constant and varied the initial concentration of the aqueous solution (Supplementary
257 information, Table SI1). Despite the differences in the total amount retained by the soil and
258 the three sand samples, over 70% of the retention occurred in the first three hours of the
259 trial, and the initial slope for the sorption was larger for the soil than for the sand samples.
260 For all the metals, the initial slope for the sorption is steep and decreases towards
261 equilibrium after the first hour. These results are similar to those obtained by Søbørg *et al.*,
262 (2019). Except in the case of Cu²⁺, adsorption in the washed sand samples (WS₁ and WS₂)
263 was lower than 50%, whereas in the RS the percentage retained varied according to the
264 metal. The lower sorption of cations in samples WS₁ and WS₂ in comparison to the soil
265 and RS can be ascribed to the carbonate content. Metal solutions were acidified to prevent
266 the hydrolysis and precipitation reactions of cations. Carbonate content in the soil and river
267 sand was enough to buffer the hydronium ions from the metal solutions, but in the case of
268 WS₁ and WS₂ samples it couldn't amortigate the acidification from metal solutions. The
269 equilibrium time of the samples ranged from 4 hours for the retention of Cu²⁺ and Cr³⁺ in
270 the soil sample to 12 hours for the retention of Cd²⁺ in the sand samples. To facilitate the
271 reproducibility of the assays, the sorption isotherms were determined after 24 hours, so that
272 the equilibrium times were reached for all the samples in all the metals analysed.

273 The shape of the adsorption isotherm is related to the energy of the interaction,

274 whereas the amount retained depends on its retention ability or monolayer capacity. Figure
275 3 depicts the isotherms of the five cations for the soil and the three sand samples. Because
276 the soil had greater capacity to retain metals than the sand, the sand sample isotherms have
277 been inserted in the graph of the soil isotherms but on a different scale. The isotherms
278 reveal differences in retention among metals, as well as among the soil and the sand
279 samples. The isotherm of Cr^{3+} in the soil belongs to type H2 of the Giles *et al.* (1960)
280 classification. These isotherms are characterized by an almost vertical slope at low
281 equilibrium concentrations, and a plateau in which the amount adsorbed scarcely varied
282 with the equilibrium concentration. The isotherms of the rest of the cations belong to group
283 L2 of the Giles classification. In these isotherms, the amount retained is proportional to the
284 equilibrium concentration in the initial part of the isotherm; the initial section is followed
285 by a knee related to the saturation of the active adsorption centers, and another section
286 whose slope reflects the soil's heterogeneity. The isotherms of the metals in the sands
287 have a lower initial slope and reach a plateau at lower equilibrium concentrations than the
288 soil, which demonstrates that they are adsorbents with limited metal cation retention
289 capacity.

290 Table 2 shows the adsorption parameters obtained when applying the Langmuir and
291 Freundlich models to experimental data from isotherms. The capacity of the monolayer,
292 n_m^a , and Freundlich's constant, k_F , are parameters related to the retention capacity, although
293 n_m^a is the amount of retention in the plateau of the isotherm and k_F is the amount retained
294 for an equilibrium concentration equal to one, in this research 1 mg L^{-1} . Despite the
295 differences observed in the magnitude of these parameters, their trends are similar for the
296 adsorbents and metals. The parameters n_m^a and k_F were much greater for the soil than for
297 the sand samples, which could be attributed to the higher proportion of clay and silt, as well
298 as to the contribution of the soil's laminar silicates. In the sand samples, RS retained more
299 metals than WS_1 and WS_2 , which might be related to its larger content in CaCO_3 . In any
300 case, the adsorption capacity of heavy metals was significantly larger in the soil than in the
301 sand samples, which is in line with the results found by other authors such as Reddy *et al.*
302 (2014).

303 The order of the quantitative retention of the cations in the soil was as follows: Cr^{3+}
304 $> \text{Cu}^{2+} > \text{Zn}^{2+} > \text{Ni}^{2+} > \text{Cd}^{2+}$. Cr^{3+} has a higher oxidation number than the rest of the ions
305 and thus it has a greater affinity for exchanging with ions like Ca^{2+} and Mg^{2+} that are present

306 in the clay-humic complex of the soil. The higher formal charge and smaller size of the
307 cation Cr^{3+} also facilitates the hydrolysis reactions that can induce precipitation in the form
308 of oxides. The steep initial slope and the sharp knee of the Cr^{3+} isotherm are typical of a
309 high interaction between adsorbent and adsorbate (Figure 3). The monolayer capacity and
310 Freundlich constant of cadmium retained by the soil was smaller than the other cations, in
311 consonance with the heavy metal retention results in soils of a different composition
312 (Echeverria *et al.*, 1998).

313 **3.3 Dynamic assays and breakthrough curves**

314 The saturated hydraulic conductivity of WS_1 was $6.23 \times 10^{-3} \pm 8.80 \times 10^{-5} \text{ cm s}^{-1}$,
315 whereas that of the soil-sand mixture was $4.33 \times 10^{-4} \pm 1.04 \times 10^{-4} \text{ cm s}^{-1}$, which is an
316 improvement of one order of magnitude. Contrasting these values with those provided by
317 Kutilek and Nielsen (1994) for the classification of soils in terms of their permeability, the
318 soil- WS_1 sand mixture had an average permeability. As expected, it was observed that the
319 conductivity values of the sand samples displayed less variability than the soil-sand
320 mixture.

321 Figure 4 shows the concentration and standard deviation, expressed in mmol/L, of
322 heavy metal ions and Ca^{2+} in the leached solution as a function of the total volume leached.
323 Two trends are shown in the concentration curves: first, Cu^{2+} and Cr^{3+} concentrations in the
324 leachate were lower than the detection limits of the experimental technique; second, Ni^{2+}
325 ions in the permeate were detected at 200 mL, and Cd^{2+} , Zn^{2+} ions at 240 mL. Therefore,
326 in the experimental conditions reported in this research, the amount of metals retained up
327 to a lixiviate volume of 200 mL would be the upper limit for SUDS. With these values of
328 the breakthrough point for each metal, the atomic masses and the initial solution
329 concentration, the retention capacities of the filter medium for each metal were as follows:
330 Cd^{2+} , 2.13 kg m^{-3} ; Zn^{2+} , 1.24 kg m^{-3} ; and Ni^{2+} , 0.97 kg m^{-3} .

331 With regard to Ca^{2+} , its leached concentration was lower than 10 mM, up to a total
332 volume of 60 mL (Fig. 4). Starting from this volume, the amount in solution increased to
333 45 mM. From there on, and throughout the assay, the concentration of Ca^{2+} in the leachate
334 diminished from 45 mM to 35 mM. These results imply that the ions of Cd^{2+} , Ni^{2+} and Zn^{2+}
335 were retained in the adsorbent mixture due to an ion exchange with the Ca^{2+} ions that
336 saturate the adsorbent's colloids.

337 Figure 5 shows the variation in pH and in ζ -Zeta as a function of the volume of
338 leachate. The pH of the lixiviate was measured to assess the buffering capacity of the soil-
339 sand mixture, given that the solution of metals had a pH 3 to prevent hydrolysis and
340 precipitation of the ions. In Figure 5 three sections can be distinguished. Up to 200 mL of
341 leachate, the pH fell to 6.5. For volumes higher than 200 mL, the pH value tended to be
342 maintained between 6.5 and 6.0. This was due to the buffering capacity of the mixture of
343 soil and sand resulting from the action of the carbonates present in the medium. From 400
344 mL upwards, the system was fed with deionized water that leached away the metal solution
345 that may have remained in the gaps of the soil/sand system. For this reason, there was a
346 general trend towards incrementing the pH of the leachate mixtures, from values of 6.0 to
347 approximately 6.75. Considering that the pH of runoff water is similar to that of rain, i.e.
348 between 5 and 5.5 for the study zone (Vet *et al.*, 2014), the acidification of the adsorbent
349 can be expected to be less than that described in the experimental conditions.

350 Figure 5 also shows the variation in ζ -Zeta (secondary axis), expressed in mV, as a
351 function of the volume of leachate. The variation in the zeta potential of the leachate
352 displays two sections. The negative charge of the colloids was neutralized when 90 mL had
353 been leached corresponding to the application of the metal solution. The rest of the ζ -Zeta
354 measurements were within the interval 0 ± 5 mV, which corresponds to the variability of
355 the deionized water blank. Therefore, the cations neutralized the negative load of the
356 colloids in the first retention stages. When the load of colloids had been neutralized, the
357 metal retention could be attributed to ion exchange or to precipitation reactions.

358 Given that Cu^{2+} and Cr^{3+} could not be detected in the leachate, it would be appropriate
359 to pose the question as to whether these ions were retained in the column and, if so, what
360 this retention mechanism is. To obtain more information, samples of the adsorbent bed
361 were taken from different sections of the column, then they were dried, and heated to mix
362 with HNO_3 and HCl in order to extract the retained metals (Ahalya *et al.*, 2003). Fig. 6
363 shows the concentration of metals retained in terms of the height of the adsorbent bed.

364 As was described in the adsorption isotherms, two adsorption trends were observed
365 in the extraction of metals from the adsorbent. The Cu^{2+} and Cr^{2+} ions were retained at a
366 higher proportion in the top 5-cm of the column, but they could not be detected in the
367 extract from the bottom of the column (20- cm). In calcareous soils, carbonated chemical

368 species control the reactivity and mobility of metals. The larger affinity of soil-Cu and soil-
369 Cr systems is in line with the first hydrolysis constant of the cations under study Cr, $pK_a =$
370 4.7; Cu, $pK_a = 7.7$; Zn, $pK_a = 9.0$; Ni, $pK_a = 9.9$; and Cd, $pK_a = 10.1$. (Basta and Tabatabai,
371 1992; Brümmer, 1986). The relation between metal sorption and cation hydrolysis suggests
372 that OH groups bind to metals in solutions and at mineral surfaces in an energetically
373 similar manner (Brady, 1992). The fact that Cu^{2+} and of Cr^{3+} were detected in the readings
374 of the leachates at the top of the column but not at the bottom suggests that both ions
375 precipitate in the column. From a design perspective, a 20-cm layer of this material would
376 be enough to reduce the load of Cu^{2+} and of Cr^{3+} to below detection limits. At the breaking
377 point, Cd^{2+} , Ni^{2+} and Zn^{2+} were homogeneously distributed throughout the height of the
378 column, with the adsorbent retention spread equally through it. So, the profile of these ions
379 in the column rules out their precipitation in the head of the adsorbent bed, and indicates
380 that they were retained by ion exchange, as is suggested by the increased leaching of
381 calcium ions.

382 The results from sorption kinetics, adsorption isotherms and breakthrough curves are
383 crucial to design systems that use soils to filter and retain contaminants in stormwater
384 management. These SUDS infiltration systems currently pose major challenges related to
385 the design, maintenance and optimization of the contaminant retention (Tedoldi *et al.*,
386 2017b). The metal input in the “Green Water Infrastructures (GWI)” implies that the soils
387 may be under a slow and persistent increase in their concentration of metals (Kabir *et al.*,
388 2014). Furthermore, given that the complex set of reaction pathways in GWIs is not fully
389 understood and characterized, it is not possible to establish *a priori* their long-term
390 retention capacities. Therefore, this research develops a method to assess the retention
391 capacity of a given soil-type to adsorb heavy metals dissolved in runoff water. Reddy *et al.*
392 (2014) and Søbørg *et al.* (2019) have characterized the properties of several materials
393 needed to adsorb contaminants under static conditions. However, we have assessed the
394 retention of metals both under static and dynamic conditions of the fluid, which provides
395 experimental data for characterizing the adsorbent and estimating the runoff volume.

396 As an example of estimating potential values of runoff volume, we applied the results
397 obtained under dynamic conditions to the filtering medium in the bioretention unit (SUDS)
398 designed in Tudela car park. The SUDS surface measures 288 m², the soil depth 30 cm and
399 it receives the runoff from a parking lot of 1,985 m². The retention capacities of the filtering

400 medium obtained for each metal are 2.13 kg of $\text{Cd}^{2+} \text{ m}^{-3}$, 1.24 kg of $\text{Zn}^{2+} \text{ m}^{-3}$ and 0.97 kg
401 of $\text{Ni}^{2+} \text{ m}^{-3}$ of adsorbent. Starting from these values, and taking into account the
402 concentration values of these metals in urban runoff in areas with a high density of traffic,
403 as compiled in the literature (Göbel *et al.*, 2007), we obtained the Total Treatable Runoff
404 Volume (TTRV) per m^3 of the adsorbent medium that the system can handle by retaining
405 each metal. We have taken the average of the maximum and minimum values from Göbel
406 *et al.* (2007) review (Table 3). Dividing the volume calculated by the surface of the parking
407 lot, and multiplying it by the surface of the SUDS, determines the height of effective
408 precipitation (EP) per meter of the medium depth that the system can handle. Finally, by
409 multiplying this value by the depth of the soil, it was obtained the value of the total effective
410 precipitation (TEP) that the soil of the SUDS can handle under ideal conditions. Table 3
411 gives all the values associated with the these calculations. Those values, along with the
412 precipitation of Cu^{2+} and of Cr^{3+} , demonstrate the great potential of the local soil for
413 retaining heavy metals. The obtained values are consistent with those published by Kabir
414 *et al.* (2014), who reported the promising capacity of GWIs to be used effectively as
415 systems for urban environment quality improvement.

416 Future research will involve extending the retention of metals under dynamic
417 conditions to soils varying in permeability and sorption capacity. Another aspect to be
418 considered in future research is which metals are adsorbed to different types of solid
419 particles, the amounts of which can end up being very significant (Borris *et al.*, 2016;
420 Gavrić *et al.*, 2019; Huber *et al.*, 2016; Loganathan *et al.*, 2013; Zafra *et al.*, 2011). These
421 particles can be retained on the surface due to sedimentation in systems like grass swales
422 or vegetative filter strips (Gavrić *et al.*, 2019; Muñoz-Carpena *et al.*, 2019). Sedimentation,
423 together with the precipitation of copper and chromium, are supported by the results
424 obtained by Tedoldi *et al.* (2017a), who showed how the vertical distribution of the
425 concentration of heavy metals in soil is characterized by a significant accumulation of them
426 on the surface, which continues decreasing with depth. Other authors like Søberg *et al.*
427 (2017) and Wang *et al.* (2017) found metals that were adsorbed in the top 5 cm of the
428 filtering material.

429 **4 CONCLUSIONS**

430 This research work has permitted the development of a technique for finding out the

431 retention capacity of heavy metals in the soil of a Sustainable Urban Drainage System
432 (SUDS), and for identifying the retention process of each metal. This has some practical
433 implications in the design and maintenance of a SUDS, as has been demonstrated.

434 The capacity of the soil to retain metal ions was far superior to that of the three sand
435 samples analysed. The order of quantitative retention of the cations in the soil was as
436 follows: $\text{Cr}^{3+} > \text{Cu}^{2+} > \text{Zn}^{2+} \approx \text{Ni}^{2+} > \text{Cd}^{2+}$. The experiments under dynamic conditions with
437 the adsorbent medium in the column made it possible to find out which metals are retained
438 at breaking point, and their retention mechanisms. The analysis of the filtering medium
439 after the assay allowed us to verify that the Cr^{3+} and Cu^{2+} ions were preferably retained in
440 the first 5 cms of the column, and that the concentration of these cations decreased to a
441 lower value than the technique's detection limit at the bottom of the column, which enables
442 one to deduce that the principal retention mechanism was precipitation. In addition, at the
443 breaking point, the concentration of Cd^{2+} , Ni^{2+} and Zn^{2+} was homogeneous throughout the
444 column, and, given that the retention was accompanied by leaching of Ca^{2+} into the
445 adsorbent bed, it can be inferred that the retention of these ions was produced mainly by
446 ion exchange.

447 **Acknowledgements**

448 This work has been financed by a research contract (OTRI 2015/021/115) between
449 the "Universidad Pública de Navarra" and the company "Navarra de Infraestructuras
450 Locales S.A." (NILSA). The authors want to thank Ana Marta Las Heras y Gregorio
451 Berrozpe, supervisors from NILSA, for their interest, support and dedication to this project.

452

453 **REFERENCES**

- 454 Ahalya, N., Ramachandra, T.V., Kanamadi, R.D., 2003. Biosorption of heavy metals. Res.
455 J. Chem. Environ. 7(4), 71–79. <https://doi.org/10.1201/9781315364339-6>
- 456 Alcántara, M.T., Gómez, J., Pazos, M., Sanromán, M.A., 2012. Electrokinetic remediation
457 of lead and phenanthrene polluted soils. Geoderma 173–174, 128–133.
458 <https://doi.org/10.1016/j.geoderma.2011.12.009>
- 459 Allabashi, R., Haile, T.M., Fuerhacker, M., Pitha, U., Scharf, B., Stach, W., Ziegenbalg,
460 F., Heidinger, S., Ertl, T., 2019. Simultaneous removal of heavy metals from synthetic

461 storm water using sustainable urban drainage systems. *Urban Water J.* 16, 444–450.
462 <https://doi.org/10.1080/1573062X.2018.1524016>

463 Andrés-Doménech, I., Perales-Momparler, S., Morales-Torres, A., Escuder-Bueno, I.,
464 2018. Hydrological performance of green roofs at building and city scales under
465 mediterranean conditions. *Sustain.* 10, 1–15. <https://doi.org/10.3390/su10093105>

466 ASTM D2434-19, 2006. Standard Test Method for Permeability of Granular Soils
467 (Constant Head), ASTM International, West Conshohocken, PA, www.astm.org.

468 Barbosa, A.E., Fernandes, J.N., David, L.M., 2012. Key issues for sustainable urban
469 stormwater management. *Water Res.* 46, 6787–6798.
470 <https://doi.org/10.1016/j.watres.2012.05.029>

471 Basta, N.T., Tabatabai, M.A., 1992. Effect of cropping systems on adsorption of metals by
472 soils: II. Effect of pH. *Soil Science* 153, 195-204.

473 Borris, M., Österlund, H., Marsalek, J., Viklander, M., 2016. Contribution of coarse
474 particles from road surfaces to dissolved and particle-bound heavy metal loads in
475 runoff: A laboratory leaching study with synthetic stormwater. *Sci. Total Environ.*
476 573, 212–221. <https://doi.org/10.1016/j.scitotenv.2016.08.062>

477 Brady, P.V., 1992. Silica surface chemistry at elevated temperatures. *Geochem.*
478 *Cosmochem. Acta.* 56, 7, 2941-2946. [https://doi.org/10.1016/0016-7037\(92\)90371-O](https://doi.org/10.1016/0016-7037(92)90371-O)

479 Bressy, A., Gromaire, M.C., Lorgeoux, C., Saad, M., Leroy, F., Chebbo, G., 2012. Towards
480 the determination of an optimal scale for stormwater quality management:
481 Micropollutants in a small residential catchment. *Water Res.*
482 <https://doi.org/10.1016/j.watres.2011.12.017>

483 Bruemmer, G.W., Gerth, J., Herms, U., 1986. Heavy metal species, mobility and
484 availability in soils. *Zeitschrift für Pflanzenernährung und Bodenkunde* 149, 382-398.
485 <https://doi.org/10.1002/jpln.19861490404>

486 Charlesworth, S.M., Nnadi, E., Oyelola, O., Bennett, J., Warwick, F., Jackson, R., Lawson,
487 D., 2012. Laboratory based experiments to assess the use of green and food based
488 compost to improve water quality in a Sustainable Drainage (SUDS) device such as a
489 swale. *Sci. Total Environ.* 424, 337–343.
490 <https://doi.org/10.1016/j.scitotenv.2012.02.075>

- 491 Crabtree, B., Moy, F., Whitehead, M., Roe, A., 2006. Monitoring pollutants in highway
492 runoff. *Water Environ. J.* 20, 287–294. <https://doi.org/10.1111/j.1747->
493 [6593.2006.00033.x](https://doi.org/10.1111/j.1747-6593.2006.00033.x)
- 494 Davis, A.P., Shokouhian, M., Sharma, H., Minami, C., 2001. Laboratory Study of
495 Biological Retention for Urban Stormwater Management. *Water Environ. Res.* 73, 5–
496 14. <https://doi.org/10.2175/106143001x138624>
- 497 Dietz, M.E., Clausen, J.C., 2008. Stormwater runoff and export changes with development
498 in a traditional and low impact subdivision. *J. Environ. Manage.* 87, 560–566.
499 <https://doi.org/10.1016/j.jenvman.2007.03.026>
- 500 Echeverria, J.C., Morera, M.T., Mazkiarin, C., Garrido, J.J., 1998. Competitive sorption of
501 heavy metal by soils. Isotherms and fractional factorial experiments. *Environ. Pollut.*
502 101, 275–284.
- 503 Eckart, K., McPhee, Z., Bolisetti, T., 2017. Performance and implementation of low impact
504 development – A review. *Sci. Total Environ.* 607–608, 413–432.
505 <https://doi.org/10.1016/j.scitotenv.2017.06.254>
- 506 Flanagan, K., Branchu, P., Boudahmane, L., Caupos, E., Demare, D., Deshayes, S., Dubois,
507 P., Meffray, L., Partibane, C., Saad, M., Gromaire, M.C., 2019. Retention and
508 transport processes of particulate and dissolved micropollutants in stormwater
509 biofilters treating road runoff. *Sci. Total Environ.* 656, 1178–1190.
510 <https://doi.org/10.1016/j.scitotenv.2018.11.304>
- 511 Fletcher, T.D., Shuster, W., Hunt, W.F., Ashley, R., Butler, D., Arthur, S., Trowsdale, S.,
512 Barraud, S., Semadeni-Davies, A., Bertrand-Krajewski, J.L., Mikkelsen, P.S., Rivard,
513 G., Uhl, M., Dagenais, D., Viklander, M., 2015. SUDS, LID, BMPs, WSUD and more
514 – The evolution and application of terminology surrounding urban drainage. *Urban*
515 *Water J.* 12, 525–542. <https://doi.org/10.1080/1573062X.2014.916314>
- 516 Fuerhacker, M., Haile, T.M., Monai, B., Mentler, A., 2011. Performance of a filtration
517 system equipped with filter media for parking lot runoff treatment. *Desalination* 275,
518 118–125. <https://doi.org/10.1016/j.desal.2011.02.041>
- 519 Garcia, R., Maiz, I., Millan, E., 1996. Heavy metal contamination analysis of roadsoils and
520 grasses from Gipuzkoa (Spain). *Environ. Technol.* 17, 763–770.

521 <https://doi.org/10.1080/09593331708616443>

522 Gavrić, S., Leonhardt, G., Marsalek, J., Viklander, M., 2019. Processes improving urban
523 stormwater quality in grass swales and filter strips: A review of research findings. *Sci.*
524 *Total Environ.* 669, 431–447. <https://doi.org/10.1016/j.scitotenv.2019.03.072>

525 Giles, C.H., MacEwan, T.H., Nakhwa, S.N., Smith, D., 1960. Studies in adsorption. Part
526 XI. A system of classification of solution adsorption isotherms, and its use in
527 diagnosis of adsorption mechanisms and in measurement of specific surface areas of
528 solids. *J. Chem. Soc.* 3973. <https://doi.org/10.1039/jr9600003973>

529 Gnecco, I., Palla, A., Sansalone, J.J., 2019. Partitioning of zinc, copper and lead in urban
530 drainage from paved source area catchments. *J. Hydrol.* 578.
531 <https://doi.org/10.1016/j.jhydrol.2019.124128>

532 Göbel, P., Dierkes, C., Coldewey, W.G., 2007. Storm water runoff concentration matrix
533 for urban areas. *J. Contam. Hydrol.* 91, 26–42.
534 <https://doi.org/10.1016/j.jconhyd.2006.08.008>

535 Hatt, B.E., Fletcher, T.D., Deletic, A., 2009. Hydrologic and pollutant removal
536 performance of stormwater biofiltration systems at the field scale. *J. Hydrol.* 365,
537 310–321. <https://doi.org/10.1016/j.jhydrol.2008.12.001>

538 Hatt, B.E., Fletcher, T.D., Deletic, A., 2008. Hydraulic and pollutant removal performance
539 of fine media stormwater filtration systems. *Environ. Sci. Technol.* 42, 2535–2541.
540 <https://doi.org/10.1021/es071264p>

541 Hatt, B.E., Siriwardene, N., Deletic, A., Fletcher, T.D., 2006. Filter media for stormwater
542 treatment and recycling: The influence of hydraulic properties of flow on pollutant
543 removal. *Water Sci. Technol.* 54, 263–271. <https://doi.org/10.2166/wst.2006.626>

544 Helmreich, B., Hilliges, R., Schriewer, A., Horn, H., 2010. Runoff pollutants of a highly
545 trafficked urban road - Correlation analysis and seasonal influences. *Chemosphere* 80,
546 991–997. <https://doi.org/10.1016/j.chemosphere.2010.05.037>

547 Hou, J., Mao, H., Li, J., Sun, S., 2019. Spatial simulation of the ecological processes of
548 stormwater for sponge cities. *J. Environ. Manage.* 232, 574–583.
549 <https://doi.org/10.1016/j.jenvman.2018.11.111>

550 Huber, M., Welker, A., Helmreich, B., 2016. Critical review of heavy metal pollution of
551 traffic area runoff: Occurrence, influencing factors, and partitioning. *Sci. Total*
552 *Environ.* 541, 895–919. <https://doi.org/10.1016/j.scitotenv.2015.09.033>

553 Jackson, M.L., Beltrán Martínez, J., 1982. *Análisis químico de suelos*. Omega.

554 Jia, H., Wang, X., Ti, C., Zhai, Y., Field, R., Tafuri, A.N., Cai, H., Yu, S.L., 2015. Field
555 monitoring of a LID-BMP treatment train system in China. *Environ. Monit. Assess.*
556 187. <https://doi.org/10.1007/s10661-015-4595-2>

557 Kabir, M.I., Daly, E., Maggi, F., 2014. A review of ion and metal pollutants in urban green
558 water infrastructures. *Sci. Total Environ.* 470–471, 695–706.
559 <https://doi.org/10.1016/j.scitotenv.2013.10.010>

560 Kandra, H.S., McCarthy, D., Fletcher, T.D., Deletic, A., 2014. Assessment of clogging
561 phenomena in granular filter media used for stormwater treatment. *J. Hydrol.* 512,
562 518–527. <https://doi.org/10.1016/j.jhydrol.2014.03.009>

563 Kutilek, M. and Nielsen, D.R., 1994. *Soil hydrology*. Catena Verlag.

564 Langmuir, I., 1918. The Adsorption of Gases on Plane Surfaces of Mica. *J. Am. Chem.*
565 *Soc.* 40 (9), 1361–1403. <https://doi.org/10.1021/ja01269a066>

566 Le Coustumer, S., Fletcher, T.D., Deletic, A., Barraud, S., Poelsma, P., 2012. The influence
567 of design parameters on clogging of stormwater biofilters: A large-scale column
568 study, *Water Research*. <https://doi.org/10.1016/j.watres.2012.01.026>

569 Lee, H., Lau, S.L., Kayhanian, M., Stenstrom, M.K., 2004. Seasonal first flush
570 phenomenon of urban stormwater discharges. *Water Res.* 38, 4153–4163.
571 <https://doi.org/10.1016/j.watres.2004.07.012>

572 Li, H., Sharkey, L.J., Hunt, W.F., Davis, A.P., 2009. Mitigation of impervious surface
573 hydrology using bioretention in North Carolina and Maryland. *J. Hydrol. Eng.* 14,
574 407–415. [https://doi.org/10.1061/\(ASCE\)1084-0699\(2009\)14:4\(407\)](https://doi.org/10.1061/(ASCE)1084-0699(2009)14:4(407))

575 Loeppert, R.H., Hallmark, C.T., Koshy, M.M., 1984. Routine procedure for rapid
576 determination of soil carbonates. *Soil Sci. Soc. Am. J.* 48, 1030–1033.
577 <https://doi.org/10.2136/sssaj1984.03615995004800050016x>

578 Loganathan, P., Vigneswaran, S., Kandasamy, J., 2013. Road-deposited sediment

579 pollutants: A critical review of their characteristics, source apportionment, and
580 management. *Crit. Rev. Environ. Sci. Technol.* 43, 1315–1348.
581 <https://doi.org/10.1080/10643389.2011.644222>

582 Ma, Y., Hao, S., Zhao, H., Fang, J., Zhao, J., Li, X., 2018. Pollutant transport analysis and
583 source apportionment of the entire non-point source pollution process in separate
584 sewer systems. *Chemosphere* 211, 557–565.
585 <https://doi.org/10.1016/j.chemosphere.2018.07.184>

586 Monrabal-Martinez, C., Meyn, T., Muthanna, T.M., 2019. Characterization and temporal
587 variation of urban runoff in a cold climate - design implications for SuDS. *Urban*
588 *Water J.* 16, 451–459. <https://doi.org/10.1080/1573062X.2018.1536758>

589 Mulligan, C.N., Yong, R.N., Gibbs, B.F., 2001. Heavy metal removal from sediments by
590 biosurfactants. *J. Hazard. Mater.* 85, 111–125. [https://doi.org/10.1016/S0304-](https://doi.org/10.1016/S0304-3894(01)00224-2)
591 [3894\(01\)00224-2](https://doi.org/10.1016/S0304-3894(01)00224-2)

592 Muñoz-Carpena, R., J.J. Lopez-Rodriguez, M.A. Campo-Bescós. 2019. Impact of the
593 uncertainty of urban soil permeability on the design and retrofitting of green areas as
594 effective vegetative filter strips to remove surface runoff heavy metals. Abstract H13I-
595 1803, AGU Annual Meeting, San Francisco, 9-13 Dec. 2019

596 Oliveira, A.D.S., Bodo, A., Beltramini Trevilato, T.M., Magosso Takayanagui, A.M.,
597 Domingo, J.L., Segura-Muñoz, S.I., 2007. Heavy metals in untreated/treated urban
598 effluent and sludge from a biological wastewater treatment plant. *Environ. Sci. Pollut.*
599 *Res.* 14, 483–489. <https://doi.org/10.1065/espr2006.10.355>

600 Reddy, K.R., Xie, T., Dastgheibi, S., 2014. Removal of heavy metals from urban
601 stormwater runoff using different filter materials. *J. Environ. Chem. Eng.* 2, 282–292.
602 <https://doi.org/10.1016/j.jece.2013.12.020>

603 Salim Akhter, M., Madany, I.M., 1993. Heavy metals in street and house dust in Bahrain.
604 *Water, Air, Soil Pollut.* 66, 111–119. <https://doi.org/10.1007/BF00477063>

605 Schiff, K.C., Tiefenthaler, L.L., Bay, S.M., Greenstein, D.J., 2016. Effects of rainfall
606 intensity and duration on the first flush from parking lots. *Water (Switzerland)* 8.
607 <https://doi.org/10.3390/w8080320>

608 Singh, B., Sekhon, G.S., 1983. Leaching of zinc, lead and cadmium in columns of

609 calcareous soils. *Zeitschrift für Pflanzenernährung und Bodenkd.* 146, 531–538.
610 <https://doi.org/10.1002/jpln.19831460414>

611 Søberg, L.C., Viklander, M., Blecken, G.T., 2017. Do salt and low temperature impair
612 metal treatment in stormwater bioretention cells with or without a submerged zone?
613 *Sci. Total Environ.* 579, 1588–1599. <https://doi.org/10.1016/j.scitotenv.2016.11.179>

614 Søberg, L.C., Winston, R., Viklander, M., Blecken, G.T., 2019. Dissolved metal adsorption
615 capacities and fractionation in filter materials for use in stormwater bioretention
616 facilities. *Water Res. X* 4, 100032. <https://doi.org/10.1016/j.wroa.2019.100032>

617 Sposito, G., 1980. Derivation of the Freundlich Equation for Ion Exchange Reactions in
618 Soils. *Soil Sci. Soc. Am. J.* 44, 652.
619 <https://doi.org/10.2136/sssaj1980.03615995004400030045x>

620 Tedoldi, D., Chebbo, G., Pierlot, D., Branchu, P., Kovacs, Y., Gromaire, M.C., 2017a.
621 Spatial distribution of heavy metals in the surface soil of source-control stormwater
622 infiltration devices – Inter-site comparison. *Sci. Total Environ.* 579, 881–892.
623 <https://doi.org/10.1016/j.scitotenv.2016.10.226>

624 Tedoldi, D., Chebbo, G., Pierlot, D., Kovacs, Y., Gromaire, M.C., 2017b. Assessment of
625 metal and PAH profiles in SUDS soil based on an improved experimental procedure.
626 *J. Environ. Manage.* 202, 151–166. <https://doi.org/10.1016/j.jenvman.2017.06.063>

627 Tedoldi, D., Chebbo, G., Pierlot, D., Kovacs, Y., Gromaire, M.C., 2016. Impact of runoff
628 infiltration on contaminant accumulation and transport in the soil/filter media of
629 Sustainable Urban Drainage Systems: A literature review. *Sci. Total Environ.* 569–
630 570, 904–926. <https://doi.org/10.1016/j.scitotenv.2016.04.215>

631 Vardhan, K.H., Kumar, P.S., Panda, R.C., 2019. A review on heavy metal pollution,
632 toxicity and remedial measures: Current trends and future perspectives. *J. Mol. Liq.*
633 290, 111197. <https://doi.org/10.1016/j.molliq.2019.111197>

634 Veith, J.A., Sposito, G., 1977. On the Use of the Langmuir Equation in the Interpretation
635 of “Adsorption” Phenomena. *Soil Sci. Soc. Am. J.* 41, 697.
636 <https://doi.org/10.2136/sssaj1977.03615995004100040015x>

637 Vet, R., Artz, R.S., Carou, S., Shaw, M., Ro, C.U., Aas, W., Baker, A., Bowersox, V.C.,
638 Dentener, F., Galy-Lacaux, C., Hou, A., Pienaar, J.J., Gillett, R., Forti, M.C., Gromov,

639 S., Hara, H., Khodzher, T., Mahowald, N.M., Nickovic, S., Rao, P.S.P., Reid, N.W.,
640 2014. A global assessment of precipitation chemistry and deposition of sulfur,
641 nitrogen, sea salt, base cations, organic acids, acidity and pH, and phosphorus. *Atmos.*
642 *Environ.* 93, 3–100. <https://doi.org/10.1016/j.atmosenv.2013.10.060>

643 Wang, J., Zhao, Y., Yang, L., Tu, N., Xi, G., Fang, X., 2017. Removal of heavy metals
644 from urban stormwater runoff using bioretention media mix. *Water (Switzerland)* 9.
645 <https://doi.org/10.3390/w9110854>

646 Zafra, C.A., Temprano, J., Tejero, I., 2011. Distribution of the concentration of heavy
647 metals associated with the sediment particles accumulated on road surfaces. *Environ.*
648 *Technol.* 32, 997–1008. <https://doi.org/10.1080/09593330.2010.523436>

649 Zinger, Y., Fletcher, T.D., Deletic, A., Blecken, G.T., Viklander, M., 2007. Optimisation
650 of the nitrogen retention capacity of stormwater biofiltration systems. *Novatech Conf.*
651 *Lyon, Fr.* 24–28.

652

653

Table 1. Content in inorganic carbon, pH, and ζ -Zeta for the sands and soil samples.

Table 2. Langmuir and Freundlich parameters deduced from the adsorption isotherms of ions Cr^{3+} , Cu^{2+} , Ni^{2+} , Zn^{2+} and Cd^{2+} by the soil and sand samples.

Table 3. Total treatable runoff volume at the SUDS from a car park in Tudela (Spain).

Table 1. Content in inorganic carbon, pH, and ζ -Zeta for the sands and soil simple.

	Inorganic C (% CaCO ₃)	pH saturation.	ζ -Zeta (mV)
Soil	34.9	7.9	-21
RS	20.1	8.4	-17
WS ₁	0.38	8.3	-20
WS ₂	0.38	8.7	-20

RS - river sand; WS₁ - washed sand 1, WS₂ - washed sand 2.

Table 2. Langmuir and Freundlich parameters deduced from the adsorption isotherms of ions Cr^{3+} , Cu^{2+} , Ni^{2+} , Zn^{2+} and Cd^{2+} by the soil and sand samples.

	Langmuir		Freundlich	
	n_m^a (mmol/kg)	B_L (L/mg)	k_F (mmol/kg)	n
Cr^{3+}				
Soil	61.3	2.63	15.4	0.176
RS	1.37	25.3	0.943	0.194
WS ₁	1.11	33.7	0.772	0.126
WS ₂	0.95	22.8	0.871	0.338
Cu^{2+}				
Soil	52.9	0.190	10.80	0.812
RS	2.00	3.14	0.93	0.571
WS ₁	5.34	1.83	1.39	0.500
WS ₂	0.42	0.83	0.09	1.09
Zn^{2+}				
Soil	24.6	1.76	8.75	0.739
RS	4.29	9.56	3.42	0.436
WS ₁	0.40	40.1	0.31	0.197
WS ₂	0.37	10.9	0.31	0.413
Ni^{2+}				
Soil	22.79	1.48	6.29	0.613
RS	1.55	13.5	1.16	0.418
WS ₁	1.42	0.81	0.44	0.760
WS ₂	1.48	0.73	0.43	0.770
Cd^{2+}				
Soil	11.4	0.69	4.36	0.945
RS	1.11	1.39	0.61	0.700
WS ₁	0.17	1.74	0.12	0.345
WS ₂	0.29	2.60	0.17	1.03

RS - river sand; WS₁ - washed sand 1, WS₂ - washed sand 2.

Table 3. Total treatable runoff volume at the SUDS from a car park in Tudela (Spain).

	BP ^a	MRC ^b	RCAM ^c	CRTA ^d (µg/L)		TTRV ^e	EP ^f	TEP ^g
	mL	g	Kg	Min	Max	L	(L/m ²)	(L/m ²)
Cd ²⁺	240	0.27	2.13	0.3	13	3.2·10 ⁸	4.64·10 ⁷	1.39 10 ⁷
Zn ²⁺	240	0.16	1.24	120	2000	1.17·10 ⁶	1.69·10 ⁵	5.08 10 ⁴
Ni ²⁺	210	0.12	0.97	4	70	2.62·10 ⁷	3.81·10 ⁷	1.14 10 ⁶

^a BP: Breaking Point

^b MRC: Metal Retained in the Column

^c RCAM: Retention Capacity per m³ of Adsorbent Medium (soil)

^d CRTA: Metal Concentration of Runoff from Trafficked Areas with high density (Göbel et al., 2007)

^e TTRV: Total Treatable Runoff Volume per m³ of adsorbent medium (soil)

^f EP: Effective Precipitation height per m of soil depth

^g TEP: Total Effective Precipitation height that the SUDS can handle

Fig. 1. Setup for the dynamic experiments on the retention of metals by a mixture of soil (70%) and sand (30%)

Fig. 2. Sorption kinetics for Cd^{2+} , Cr^{3+} , Cu^{2+} , Ni^{2+} and Zn^{2+} by the soil and sand samples (RS, WS_1 and WS_2)

Fig. 3. Sorption isotherms at 25 °C for the retention of Cr^{3+} , Cu^{2+} , Ni^{2+} , Zn^{2+} and Cd^{2+} by the soil and sand samples (RS, WS_1 and WS_2). The plots include the isotherm type for the soil according to Giles et al. (1960) classification: H, high affinity; L, Lagmuir.

Fig. 4. Concentration of heavy metals and calcium in solution as a function of leached volume.

Fig. 5. Variation of pH and ζ -Zeta as a function of the volume of lixivate.

Fig. 6. Concentration of metals as a function of height for the sampling column.

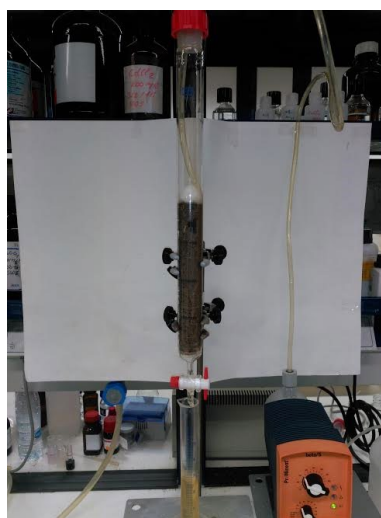


Fig. 1. Setup for the dynamic experiments on the retention of metals by a mixture of soil (70%) and sand (30%).

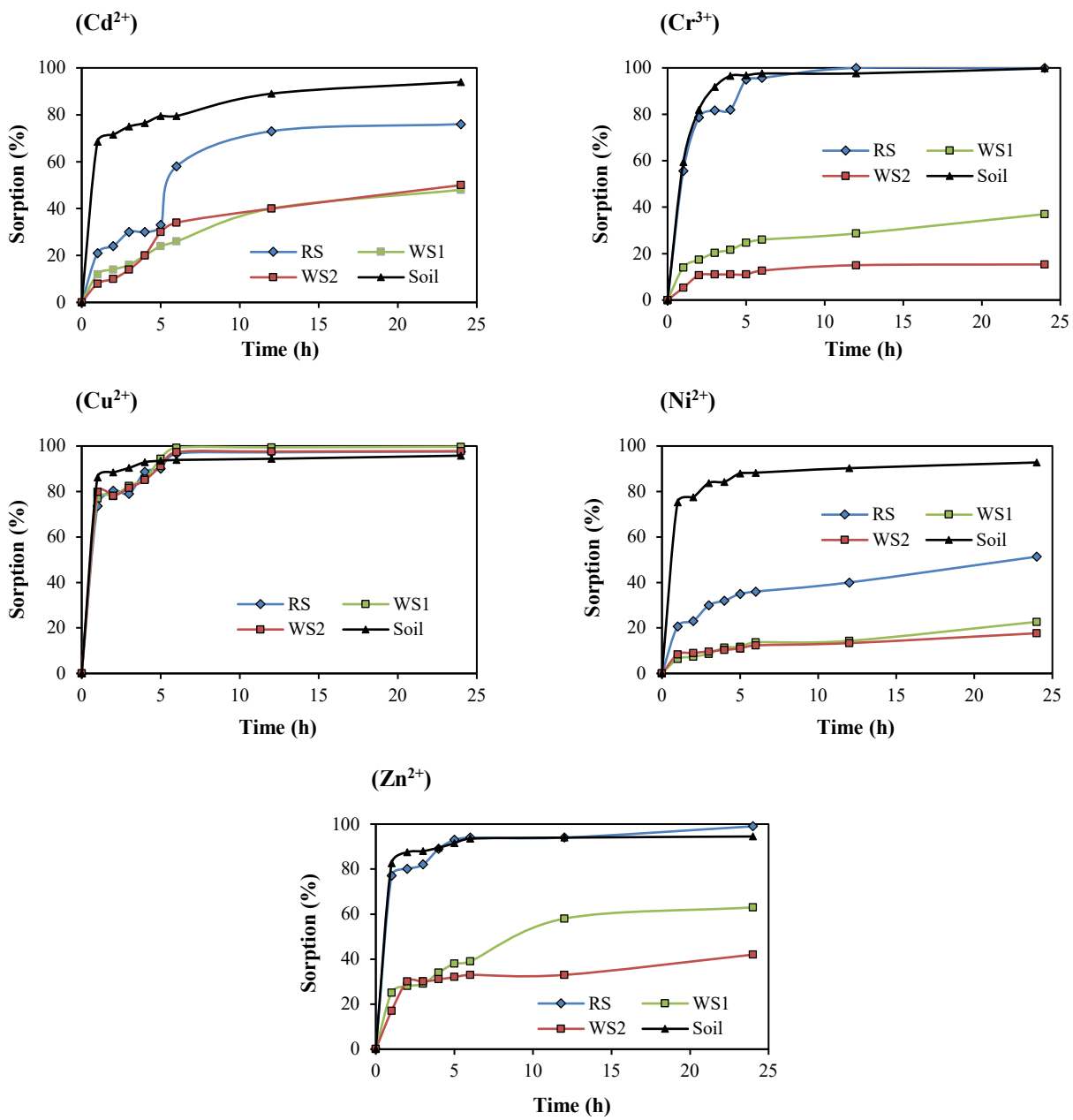


Fig. 2. Sorption kinetics for Cd²⁺, Cr³⁺, Cu²⁺, Ni²⁺ and Zn²⁺ by the soil and sand samples (RS, WS₁ and WS₂).

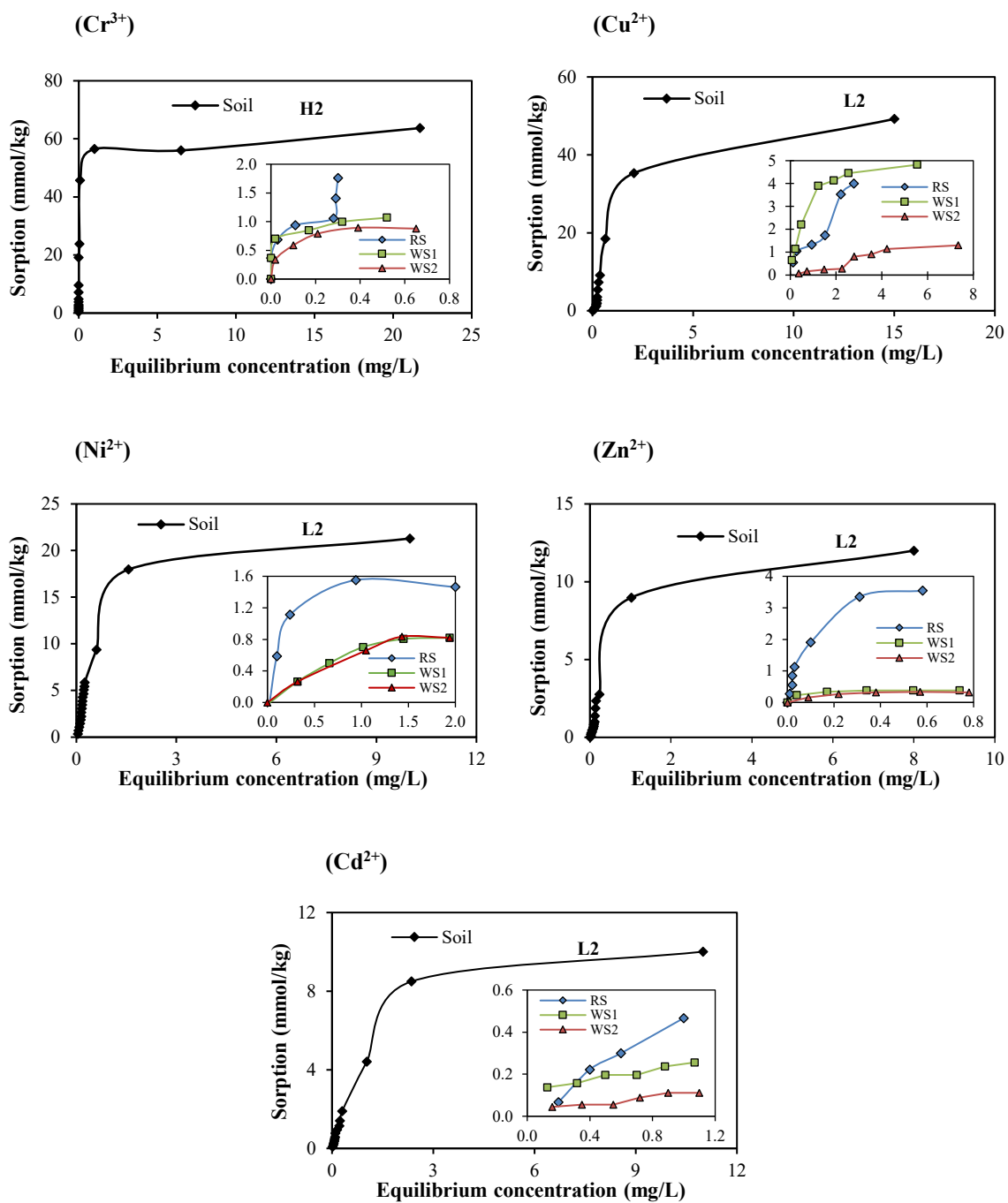


Fig. 3. Sorption isotherms at 25 °C for the retention of Cr^{3+} , Cu^{2+} , Ni^{2+} , Zn^{2+} and Cd^{2+} by the soil and sand samples (RS, WS₁ and WS₂). The plots include the isotherm type for the soil according to Giles et al. (1960) classification: H, high affinity; L, Lagmuir.

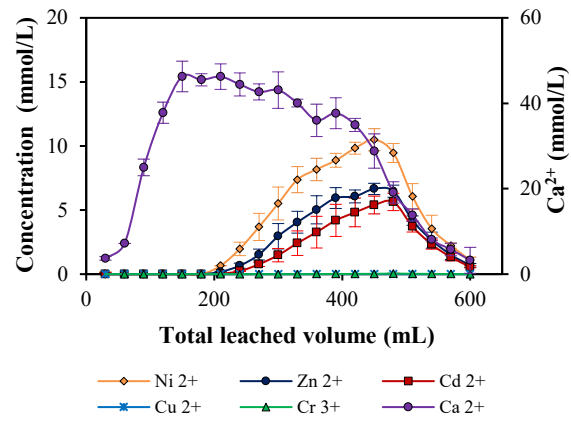


Fig. 4. Concentration of heavy metals and calcium in solution as a function of leached volume.

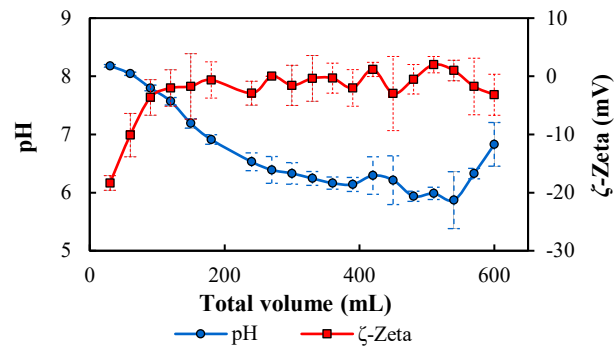


Fig. 5. Variation of pH and ζ -Zeta as a function of the volume of lixivate.

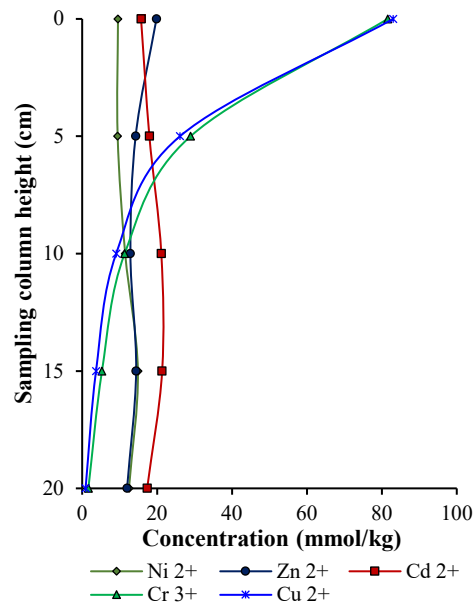


Fig. 6. Concentration of metals as a function of height for the sampling column.